

Extraction of nucleus-nucleus potential and energy dissipation from dynamical mean-field theory

Kouhei Washiyama and Denis Lacroix

GANIL, BP55027, 14076 Caen, France

Abstract. Nucleus-nucleus interaction potentials in heavy-ion fusion reactions are extracted from the microscopic time-dependent Hartree-Fock theory. When the center-of-mass energy is much higher than the Coulomb barrier energy, extracted potentials identify with the frozen density approximation. As the center-of-mass energy decreases to the Coulomb barrier energy, potentials become energy dependent. This dependence indicates dynamical reorganization of internal degrees of freedom and leads to a reduction of the "apparent" barrier. Including this effect leads to the Coulomb barrier energy very close to experimental one. Aspects of one-body energy dissipation extracted from the mean-field theory are discussed.

Keywords: TDHF, fusion reaction, classical trajectory, macroscopic dissipative equation, dynamical effect, energy dependence of nucleus-nucleus potential, one-body energy dissipation

PACS: 25.70.Jj, 21.60.Jz

INTRODUCTION

The interplay between nuclear structure and dynamical effects is crucial to properly describing fusion reactions at energies close to the Coulomb barrier. Coupled-channels models [1, 2] have been widely used to describe the entrance channel of fusion reactions. While in general rather successful, these models have in common several drawbacks. First, nuclear structure and dynamical effects should be treated in a unified framework. Second, important channels should be guessed *a priori*. Mean-field theories based on the Skyrme energy density functional provide a rather unique tool for describing nuclear structure and nuclear reactions in a unified framework, i.e., all of the dynamical coupling effects between collective and intrinsic degrees of freedom. In nuclear reactions, application of the time-dependent Hartree-Fock (TDHF) to heavy-ion fusion reactions was a major step [3, 4, 5, 6]. Since recent TDHF calculations can now include all terms of the Skyrme energy density functional used in static Hartree-Fock calculations [7, 8, 9, 10], the description of nuclear reactions using TDHF should be revisited.

In this contribution, as one of the applications of TDHF to nuclear reactions, we propose a method for simultaneously extracting nucleus-nucleus potentials and friction coefficients associated with one-body energy dissipation from the microscopic TDHF theory [11]. In this method, we assume that fusion dynamics is described by one-dimensional macroscopic dissipative dynamics on the relative distance between colliding nuclei. In order to validate our assumption, we first compare extracted potential with alternative mean-field methods [12, 13]. Then, we discuss the property of nucleus-nucleus potential and one-body energy dissipation deduced from TDHF.

METHOD

The potential and friction coefficient of one-body energy dissipation are extracted as follows: (i) The TDHF equation of head-on collision is solved to obtain the time evolution of the total density of colliding nuclei. (ii) After dividing the total density into two densities at the separation plane defined in Ref. [11], we compute at each time different macroscopic variables: relative distance R , associated momentum P , and reduced mass μ . (iii) We assume that the time evolutions of R and P obey a classical equation of motion including a friction term which depends on the velocity \dot{R} :

$$\frac{dR}{dt} = \frac{P}{\mu}, \quad \frac{dP}{dt} = -\frac{dV}{dR} - \gamma(R)\dot{R}, \quad (1)$$

where $V(R)$ and $\gamma(R)$ denote the nucleus-nucleus potential and friction coefficient, respectively. The friction coefficient $\gamma(R)$ describes the effect of energy dissipation from the macroscopic degrees of freedom to the microscopic ones. (iv) Equation (1) has two unknown quantities dV/dR and $\gamma(R)$. These quantities are obtained by using two TDHF evolutions with slightly different energies [11]. The potential $V(R)$ is deduced by integration over R using its asymptotic Coulomb potential at large relative distances. For the TDHF calculations, the three-dimensional TDHF code developed by P. Bonche and coworkers with the SLy4d Skyrme effective force [7] is used. The mesh sizes in space and in time are 0.8 fm and 0.45 fm/c, respectively. This method is called hereafter dissipative-dynamics TDHF (DD-TDHF).

NUCLEUS-NUCLEUS POTENTIAL

Comparison of potential

The present method assumes that the mean-field dynamics can properly be reduced to a one-dimensional macroscopic dissipative equation. In order to validate this assumption, we first compare the potential that we obtained, denoted by V^{DD} , with other techniques based on mean-field theories.

The potential $V^{DD}(R)$ is displayed by the solid line in Fig 1 for the $^{16}\text{O}+^{16}\text{O}$ reaction at the center-of-mass energy $E_{c.m.} = 34$ MeV. The potentials obtained by the density-constrained TDHF (DC-TDHF) method [12] (dashed line) and by the frozen-density (FD) approximation [13] (filled circles-dotted line) are also shown for comparison. In DC-TDHF, dynamical effects are partially accounted for by minimizing at each time step the total energy under the constraint of the density reached along the TDHF path. The FD approximation is based on the sudden approximation and estimates potential energy from energy density functional with the condition that projectile and target densities are frozen to their respective ground state densities at each R . Figure 1 shows that the potentials extracted from DD-TDHF and from DC-TDHF are almost identical even well inside the Coulomb barrier. This gives confidence in the specific macroscopic equation [Eq. (1)] retained to reduce the microscopic dynamics. In addition, both methods are almost identical to the FD approximation (for $R \geq 6.5$ fm). This indicates that little

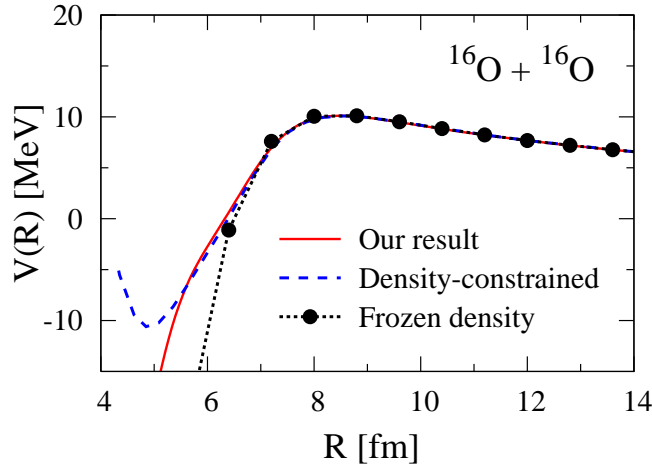


FIGURE 1. Comparison of potential energies for the $^{16}\text{O}+^{16}\text{O}$ reaction obtained from different models. The solid, dashed, and filled circles-dotted lines correspond to our result, to the density-constrained method [12], and to the frozen density approximation [13], respectively.

reorganization of densities occurs in the approaching phase at this energy ($E_{\text{c.m.}} = 34$ MeV), which is well above the Coulomb barrier energy. As a consequence, the Coulomb barrier predicted by TDHF is almost identical to the one obtained in the FD case (the difference being less than 0.1 MeV). It is worth mentioning that our method assumes neither sudden nor adiabatic approximation.

Energy dependence of extracted potential

To illustrate the center-of-mass energy dependence of the potential, Fig. 2 presents potentials obtained with DD-TDHF using several center-of-mass energies ranging from $E_{\text{c.m.}} = 55$ MeV to 100 MeV for the $^{40}\text{Ca}+^{40}\text{Ca}$ reaction. Again, in the high energy limit, potentials identify with the FD case. In addition, an increase of center-of-mass energy from $E_{\text{c.m.}} = 90$ to 100 MeV leads to identical results indicating the stability of DD-TDHF as the energy increases. In opposite, as $E_{\text{c.m.}}$ decreases, potentials deduced from DD-TDHF deviates from the FD case. As $E_{\text{c.m.}}$ approaches the Coulomb barrier energy, a small change in $E_{\text{c.m.}}$ significantly affects extracted potential as illustrated by the two energies $E_{\text{c.m.}} = 55$ MeV and 57 MeV shown in Fig. 2.

This effect is a direct consequence of reorganization of densities in the approaching phase. This is clearly illustrated in Fig. 3 where density profiles obtained for the $^{40}\text{Ca}+^{40}\text{Ca}$ reaction at $E_{\text{c.m.}} = 55$ and 90 MeV are shown for specific R values. In Fig. 3, only the case of $E_{\text{c.m.}} = 90$ MeV resembles the FD case, remaining spherical. At low energy $E_{\text{c.m.}} = 55$ MeV, a clear deviation from the FD profile is observed. As the two partners approach, deformation of the two nuclei takes place. This deformation initiates the formation of a neck at larger relative distances compared to $E_{\text{c.m.}} = 90$ MeV. This center-of-mass energy dependence of the extracted potential reflects the difference in the density profiles accessed dynamically during the mean-field evolution. Note that similar

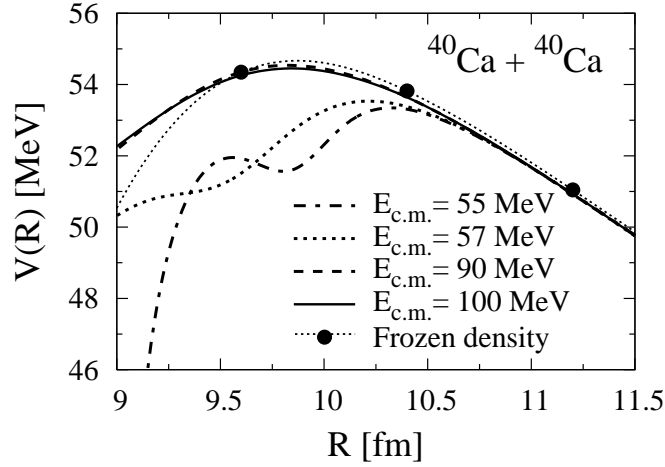


FIGURE 2. Potential energy for the $^{40}\text{Ca}+^{40}\text{Ca}$ reaction extracted at different center-of-mass energies. The FD potential is shown by the filled circles-dotted line.

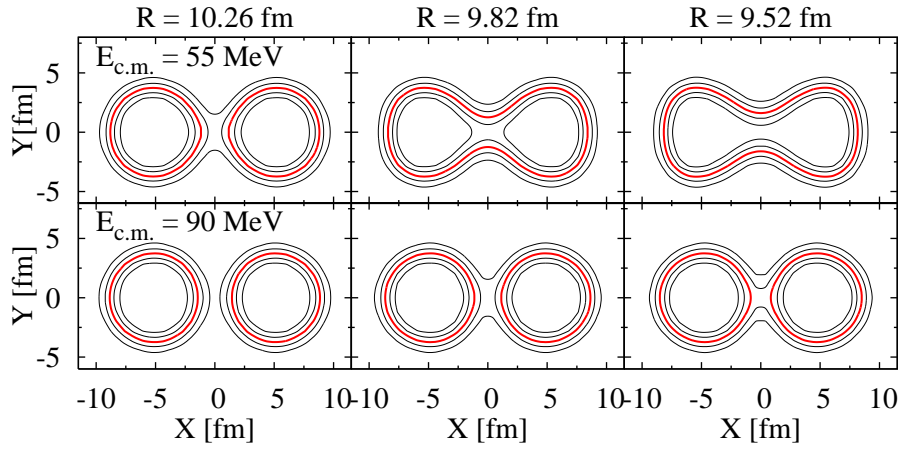


FIGURE 3. Density profiles obtained from TDHF for different relative distances $R = 10.26$ (left), 9.82 (middle), and 9.52 fm (right) for the $^{40}\text{Ca}+^{40}\text{Ca}$ reaction at $E_{c.m.} = 55$ (top) and 90 MeV (bottom).

dependence is *a priori* also expected in the DC-TDHF method [12, 14], which accounts for the dynamical deformation of the densities.

Dynamical effect on extracted potentials is systematically found in all reactions considered here. Figure 4 shows the difference between the barrier height deduced from DD-TDHF and the barrier height from experiment [15] as a function of extracted barrier height for the $^{16}\text{O}+^{40}\text{Ca}$, $^{40,48}\text{Ca}+^{40,48}\text{Ca}$, $^{16}\text{O}+^{208}\text{Pb}$, and $^{40}\text{Ca}+^{90}\text{Zr}$ reactions. The solid line is the result when potential barrier is extracted in the high energy limit of DD-TDHF ($E_{c.m.} \gg V_B$), whereas the dashed line for the low energy limit of DD-TDHF ($E_{c.m.} \sim V_B$). Dynamical reduction of the barrier energy is clearly seen for all the reactions. Moreover, the value of the barrier energy approaches the experimental data. This underlines the importance of dynamical effects close to the Coulomb barrier and illustrates the degree of precision of our technique.

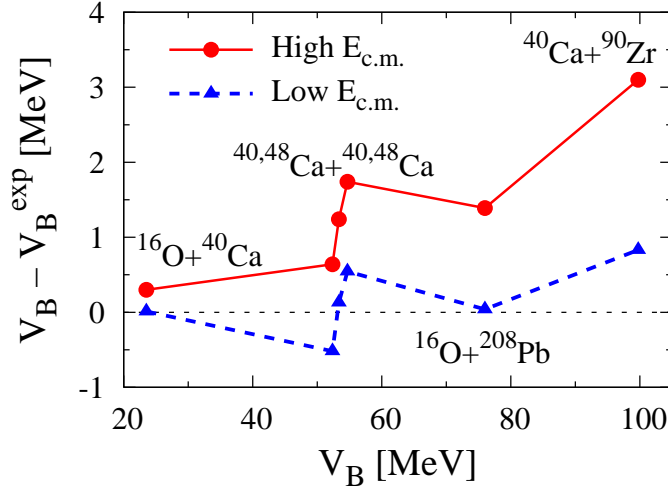


FIGURE 4. Difference between the barrier height deduced from DD-TDHF and experimental barrier height [15] as a function of extracted barrier height for the reactions indicated in the figure. V_B is deduced from high energy TDHF (solid line) and from low energy TDHF (dashed line).

FRICION COEFFICIENT FROM MICROSCOPIC MEAN-FIELD

In most practical models with dissipation applied to nuclear reactions at energies around the Coulomb barrier, the mechanism of energy dissipation is assumed to be of one-body type, where energy dissipation is caused by collision of nucleons with the wall of mean-field potential and by nucleon exchange between colliding nuclei, i.e., the so-called wall-and-window formula [16, 17, 18]. TDHF includes the mechanism of one-body energy dissipation from the microscopic point of view because of the self-consistency of mean-field. Therefore, we investigate the property of energy dissipation from the microscopic point of view by DD-TDHF [19].

In Fig. 5, we present reduced friction parameters defined as $\beta(R) = \gamma(R)/\mu(R)$ as a function of R scaled by the Coulomb barrier radius R_B . As the colliding nuclei approach, the magnitude of the friction coefficients monotonically increases. Figure 5 clearly shows that the order of magnitude of $\beta(R)$ and the radial dependence are almost independent on the size and asymmetry of the system. Besides, we compare our results with a microscopic model [20] based on the linear response theory by the filled-circles. They agree very well. DD-TDHF gives energy dissipation in reasonable order of magnitude and points out that extracted friction coefficients have universal behavior.

SUMMARY

A novel method (DD-TDHF) based on the macroscopic reduction of TDHF has been used to extract nucleus-nucleus potential as well as one-body energy dissipation. The DD-TDHF gives important insight in the dynamical effects and provides a way to extract friction coefficient from dynamical microscopic theory.

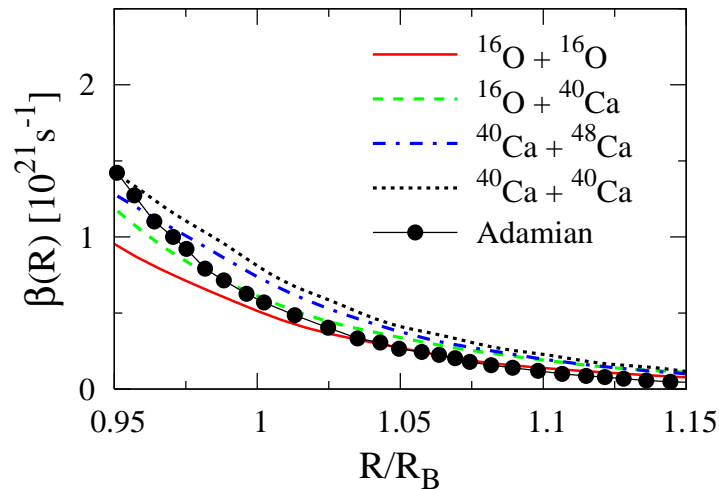


FIGURE 5. Extracted reduced friction parameter $\beta(R) = \gamma(R)/\mu(R)$ as a function of R scaled by the Coulomb barrier radius R_B for several reactions. A microscopic friction by Adamian *et al.* [20] is shown by the filled-circles for comparison.

ACKNOWLEDGMENTS

We thank P. Bonche for providing his TDHF code and S. Ayik for fruitful discussions.

REFERENCES

1. A. B. Balantekin and N. Takigawa, *Rev. Mod. Phys.* **70**, 77 (1998).
2. M. Dasgupta, D. J. Hinde, N. Rowley, and A. M. Stefanini, *Annu. Rev. Nucl. Part. Sci.* **48**, 401 (1998).
3. P. Bonche, S. E. Koonin, and J. W. Negele, *Phys. Rev. C* **13**, 1226 (1976).
4. H. Flocard, S. E. Koonin, and M. S. Weiss, *Phys. Rev. C* **17**, 1682 (1978).
5. S. E. Koonin, *Prog. Part. Nucl. Phys.* **4**, 283 (1980).
6. J. W. Negele, *Rev. Mod. Phys.* **54**, 913 (1982).
7. K.-H. Kim, T. Otsuka, and P. Bonche, *J. Phys. G* **23**, 1267 (1997).
8. T. Nakatsukasa and K. Yabana, *Phys. Rev. C* **71**, 024301 (2005).
9. A. S. Umar and V. E. Oberacker, *Phys. Rev. C* **73**, 054607 (2006).
10. J. A. Maruhn, P.-G. Reinhard, P. D. Stevenson, and M. R. Strayer, *Phys. Rev. C* **74**, 027601 (2006).
11. K. Washiyama and D. Lacroix, *Phys. Rev. C* **78**, 024610 (2008).
12. A. S. Umar and V. E. Oberacker, *Phys. Rev. C* **74**, 021601(R) (2006).
13. V. Y. Denisov and W. Nörenberg, *Eur. Phys. J. A* **15**, 375 (2002).
14. A. S. Umar and V. E. Oberacker, *Phys. Rev. C* **74**, 061601(R) (2006); *Phys. Rev. C* **76**, 014614 (2007).
15. J. O. Newton, R. D. Butt, M. Dasgupta, D. J. Hinde, I. I. Gontchar, C. R. Morton, and K. Hagino, *Phys. Lett.* **B586**, 219 (2004); *Phys. Rev. C* **70**, 024605 (2004).
16. J. Blocki, Y. Boneh, J. R. Nix, J. Randrup, M. Robel, A. J. Sierk, and W. J. Swiatecki, *Ann. Phys. (N.Y.)* **113**, 330 (1978).
17. J. Randrup and W. Swiatecki, *Ann. Phys. (N.Y.)* **125**, 193 (1980).
18. J. Randrup and W. Swiatecki, *Nucl. Phys.* **A429**, 105 (1984).
19. K. Washiyama, D. Lacroix, and S. Ayik, in preparation.
20. G. G. Adamian, R. V. Jolos, A. K. Nasirov, and A. I. Muminov, *Phys. Rev. C* **56**, 373 (1997).